

Polymerized Pickering HIPEs: Effects of Synthesis Parameters on Porous Structure

INNA GUREVITCH, MICHAEL S. SILVERSTEIN

Department of Materials Engineering, Technion—Israel Institute of Technology, Haifa 32000, Israel

Received 2 November 2009; accepted 19 December 2009

DOI: 10.1002/pola.23911

Published online in Wiley InterScience (www.interscience.wiley.com).

ABSTRACT: A polyHIPE is a highly porous polymer synthesized from monomers within the external phase of a high internal phase emulsion (HIPE). The large amount of difficult to remove surfactant needed for HIPE stabilization can affect the properties of the resulting polymer. A Pickering emulsion is a surfactant-free emulsion stabilized by solid particles that preferentially migrate to the interface. In this article, the synthesis of crosslinked polyacrylate polyHIPEs based on Pickering HIPEs stabilized using silane-modified silica nanoparticles is described and the effects of the synthesis parameters on the porous structure are discussed. The silane chemistry, silane content, and nanoparticle content had significant effects on the size of the polyhedral, relatively closed-cell polyHIPE voids that resulted from aqueous-phase initiation. Increasing the mixing

intensity reduced the wall thickness and produced a more open-cell structure. The locus of initiation had a significant effect on polyHIPE morphology. Organic-phase initiation yielded larger, more spherical voids from the more extensive coalescence before the structure could be “locked-in” at the gel point. Most significantly, the nanoparticles were located within the polymer walls rather than at the interface, as might be expected. The void walls were shown to be an assembly of nanoparticle agglomerate shells that become embedded within the polymer. © 2010 Wiley Periodicals, Inc. *J Polym Sci Part A: Polym Chem* 48: 1516–1525, 2010

KEYWORDS: nanocomposites; polyacrylate; polyHIPE; surfaces; surfactants

INTRODUCTION PolyHIPEs are highly porous polymers synthesized from high internal phase emulsions (HIPEs), emulsions with internal phase volumes that are greater than 74% and can be greater than 90%. Typically, a polyHIPE is based on the polymerization of hydrophobic monomers and cross-linking comonomers within the continuous phase of a water-in-oil (w/o) HIPE, followed by the removal of the internal phase.^{1–4} A variety of polyHIPEs and polyHIPE-based materials have been synthesized including copolymers,^{5,6} interpenetrating polymer networks (IPN),⁷ hydrogels (using oil-in-water HIPEs),^{8,9} biocompatible polymers,^{10,11} organic-inorganic hybrids,^{12,13} and composites.^{14–21} These lightweight materials with micrometer-to-nanometer scale open-pore structures have exhibited potential as filtration media, supports for catalytic reactions, absorbents, ion-exchange systems, scaffolds for tissue engineering, and insulating foams.^{1–3,22–31}

HIPEs are formed from two highly immiscible liquids (usually water and a highly hydrophobic liquid) in the presence of a surfactant that is insoluble in the internal phase. The amount of surfactant needed for stabilization can often reach up to 30 wt % of the external phase because, in many cases, an overwhelming amount of the major phase must be dispersed within the minor phase. The porous morphology and

properties of a polyHIPE are strongly influenced by the type and amount of surfactant. Surfactants are often difficult to remove, and costly to remove. These disadvantages become more acute for polyHIPEs where unusually large quantities of surfactant are used. Surfactants have been shown to affect the properties of the resulting polymer.^{3,4} Replacing the surfactants in HIPEs should prove advantageous, especially for the synthesis of polyHIPEs.³²

A Pickering emulsion is a surfactant-free emulsion stabilized by micrometer- or nanometer-scale solid particles that preferentially migrate to the interface between the two liquid phases.^{33–38} Whereas amphiphilic surfactants reduce the oil-water interfacial tension, the solid particles form rigid shells that surround the dispersed phase and prevent coalescence.³³ The particles' shape and size, interparticle interactions, and the wetting of the particles by the liquids affect its ability to stabilize emulsions.³⁴ The stability of Pickering emulsions based on inorganic particles can be enhanced by modifying the particle surfaces with organic molecules that increase their tendency to migrate to the interface.^{34–38} The contact angle at the oil-particle-water interface determines its ability to stabilize o/w or w/o emulsions.³⁵

Several different surface modification methodologies, including silane modification, have been used to change the

Correspondence to: M. S. Silverstein (E-mail: michael.s@tx.technion.ac.il)

Journal of Polymer Science: Part A: Polymer Chemistry, Vol. 48, 1516–1525 (2010) © 2010 Wiley Periodicals, Inc.

hydrophilic nature of the surface of silica nanoparticles such that they are able to stabilize Pickering emulsions.^{35,37,39} Silane coupling agents are commonly used to enhance fiber/matrix adhesion in polymer composites.^{40,41} Alkoxysilanes and chlorosilanes contain groups that bond covalently with silica through reaction with the hydroxyl groups on its surface. These silanes also contain hydrophobic organic groups that decrease surface hydrophilicity.^{40–43} Silane-modification thus enhances the amphiphilic character of the surface, making it more suitable for Pickering emulsion stabilization. The extent of silica surface reaction with methylchlorosilane was demonstrated to affect the degree of hydrophobicity and to determine whether it would stabilize a o/w or a w/o Pickering emulsion.³⁵ In addition to controlling surface hydrophobicity, a silane that bears a vinyl group can act as a comonomer during a free radical polymerization reaction.⁴⁰

Surfactant-free Pickering HIPEs stabilized using titania and silica nanoparticles whose surfaces were modified with oleic acid have been reported.^{32,44} The nanoparticles, whose content was varied from 1 to 5 wt % (based on the monomer mass), were able to stabilize HIPEs containing up to 92 wt % internal phase. Similarly, 0.4 wt % oxidized carbon nanotubes were used to stabilize HIPEs containing up to 60 wt % internal phase⁴⁵ and poly(methyl methacrylate) microgel particles were used to stabilize HIPEs containing 50 wt % internal phase.⁴⁶ The advantages of using Pickering HIPEs are the small amount of nanoparticles used, eliminating the procedures used to remove the surfactant, and not having residual surfactant in the polyHIPE which could leach out during use. Such polyHIPEs based on Pickering HIPEs could be used to replace conventional polyHIPEs that may contain residual surfactant. Most of the polyHIPEs synthesized from these Pickering HIPEs exhibited relatively large voids (300–400 μm). Voids of around 50 μm in diameter resulted when poly(styrene-co-methyl methacrylate-co-acrylic acid) particles were used to stabilize a Pickering HIPE.⁴⁷ PolyHIPEs from Pickering HIPEs do not usually exhibit the highly porous interconnected structures typical of conventional polyHIPEs.

In this article, the synthesis of crosslinked polyacrylate polyHIPEs based on Pickering HIPEs stabilized using silane-modified silica nanoparticles are described. The effects of the nanoparticle content, the silane content, the silane's chemical structure, the intensity of mixing, and the locus of initiation on the porous structure are discussed and the cross-sectional nanostructure of the void walls is depicted.

EXPERIMENTAL

Materials

The monomer used was 2-ethylhexyl acrylate (EHA, Aldrich) and the crosslinking comonomer was divinyl benzene (DVB, containing 20% ethylstyrene, Aldrich). The monomers were washed to remove the inhibitor (thrice with a 5 wt % sodium hydroxide solution and then thrice with deionized water). The organic surfactant used for the formation of reference HIPEs was sorbitan monooleate (SMO, Span 80, Fluka Chemie). The water-soluble initiator was potassium persulfate ($\text{K}_2\text{S}_2\text{O}_8$, Riedel-de-Haen) and the organic-soluble initia-

tor was benzoyl peroxide (BPO, Fluka Chemie). The HIPE stabilizer salt was potassium sulfate (K_2SO_4 , Frutarom, Israel). Toluene (Bio Lab) was added to the organic phase as a porogen to increase pore interconnectivity and to enhance methyl methacrylate (MMA, Aldrich) infiltration for transmission electron microscopy (TEM) specimen preparation. Methanol (Bio Lab) was used for Soxhlet extraction. Deionized water was used throughout. KBr was used in the production of pellets for Fourier transform infrared spectroscopy (FTIR) (spectral grade, Riedel-de-Haen).

The silica nanoparticles had an average diameter of 7 nm and a surface area of 390 m^2/g (Sigma). The surface modifications were carried out using ethanol (Bio Lab) and acetic acid (100%, Merck). The alkoxysilane coupling agents had either a functionality of two (dimethoxysilane) or three (trimethoxysilane) and bore various organic groups. The silanes used were: 3-(methacryloxy)propyltrimethoxysilane (**a**, MPtMS, Gelest), 3-(acryloxy)propyltrimethoxysilane (**b**, APtMS, Gelest), vinyl trimethoxysilane (**c**, VtMS, Aldrich), styrylethyl trimethoxysilane (**d**, StMS, Gelest), 3-(methacryloxy)propylmethyldimethoxysilane (**e**, MPdMS, Gelest), and 3-(*n*-allylamino)propyltrimethoxysilane (**f**, AAPtMS, Gelest). The chemical structures of the silanes are presented in Figure 1.

Silane Modification

An ethanol/water solution (95 vol % ethanol) and an aqueous acetic acid solution (5.5 vol % acetic acid, 1M) were prepared. The pH of the ethanol solution was adjusted to 4.5 by adding 3 vol % of the acetic acid solution. An alkoxysilane was then added to the ethanol/acetic acid solution with the mass ratio of silane to silica nanoparticles, r_m , varied from 0 to 10.6. After the alkoxysilane in the solution underwent hydrolysis and condensation for 1 h, 1.4 wt % (relative to the solution) silica nanoparticles were added and the mixture was vigorously stirred for 0.5 h. The particles were filtered with Whatman No. 1 filter paper through a Buchner funnel and dried overnight at 70 °C in a convection oven.

Conventional PolyHIPEs

Two reference samples were synthesized using conventional polyHIPE synthesis. The first reference sample was S0, where the "0" indicates the absence of silica nanoparticles. The organic phase consisted of monomer (80 vol % EHA and 20 vol % DVB) and surfactant. The surfactant content was around 28 wt % of the monomer content. The aqueous phase, 83.3 vol % of the HIPE, consisted of water, stabilizer salt, and initiator. The second reference sample was S0-B, where the suffix "B" indicates organic-phase initiation. For organic-phase initiation, BPO was added to the organic phase and KPS was not added to the aqueous phase. The same overall mass fraction of initiator was used, whether it was BPO or KPS. The recipes for S0 and S0-B are listed in Table 1.

The aqueous phase was slowly added to the organic phase with continuous stirring. The HIPE was covered with aluminum foil and polymerized in a circulating air oven at 65 °C for 24 h without stirring. The polyHIPE was dried in a

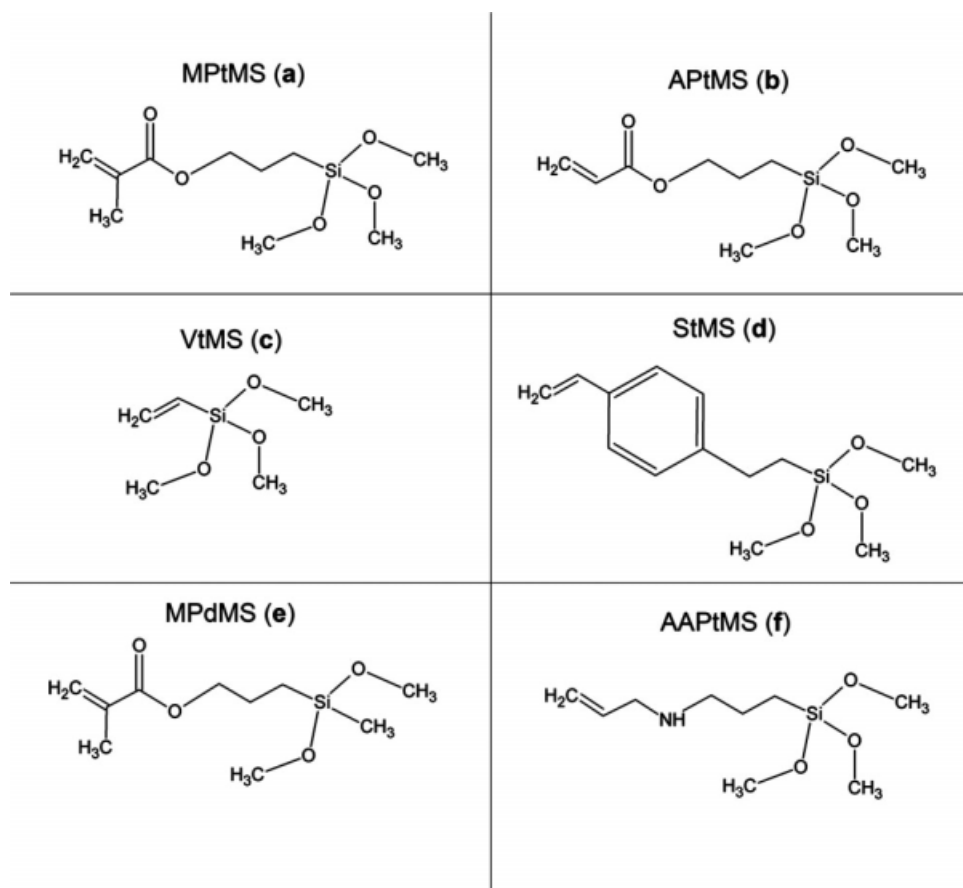


FIGURE 1 Chemical structures of silanes used in the silica surface modifications.

vacuum oven for 48 h, until a constant weight was achieved. The initiator, stabilizer salt, and surfactant were removed by Soxhlet extraction in deionized water for 24 h and then in methanol for an additional 24 h. The polyHIPE was then dried in a vacuum oven for 24 h.

Polymerized Pickering HIPEs

The synthesis procedure is almost exactly the same as for conventional polyHIPEs except for three things: (1) No sur-

factant was added to the organic phase; (2) silane-modified silica nanoparticles were added to the organic phase; (3) there was no Soxhlet extraction in methanol. The nanoparticle content varied from 2 to 7 wt % of the monomer mass. The polymerized Pickering HIPEs (PPHIPEs) are labeled “S_xyz”, where “S” denotes silica nanoparticles, *x* denotes the mass fraction of silica nanoparticles relative to the mass of monomers, *y* denotes the alkoxy silane (the **a**, **b**, **c**, or **d** in Fig. 1), and *z* is the alkoxy silane to nanoparticle mass ratio

TABLE 1 Recipes for Selected HIPEs (r_m of 1.8)

Phase	Component	Amount (wt %)				
		S0	S0-B	S4-a1.8	S4-a1.8-B	S4-a1.8-T
External	EHA	11.5	11.5	11.9	11.9	8.4
	DVB	3.0	3.0	3.1	3.1	2.1
	SMO	4.0	4.0	0	0	0
	BPO	0	0.2	0	0.2	0
	Silica	0	0	0.6	0.6	0.6
	Toluene	0	0	0	0	4.4
	Total	18.5	18.6	15.6	15.7	15.6
Internal	Water	81.0	81.0	83.9	83.9	83.9
	KPS	0.2	0	0.2	0	0.2
	Stabilizer	0.4	0.4	0.4	0.4	0.4
	Total	81.5	81.4	84.4	84.3	84.4

TABLE 2 Silica Nanoparticle Contents in the HIPEs

HIPE	Silica (wt %)	Silica (vol %)	Silane	r_m
S0	0	0	–	–
S0-B	0	0	–	–
S4-a1.0	4.2	1.7	MPtMS	1.0
S4-a1.8/-B/-T/-S	4.2	1.7	MPtMS	1.8
S4-b1.8	4.2	1.7	APtMS	1.8
S4-c1.8	4.2	1.7	VtMS	1.8
S4-d1.8	4.2	1.7	StMS	1.8
S4-a3.6	4.2	1.7	MPtMS	3.6
S7-a1.8	7.0	2.8	MPtMS	1.8

used. The suffix “B” indicates organic-phase initiation. Several example Pickering HIPE recipes are listed in Table 1. The nanoparticle contents for the various PPHIPEs are listed in Table 2. The polyHIPEs were stirred using a magnetic stirrer, which was set to its maximum of 200 rpm. The suffix “S” indicates a more intensively stirred HIPE with a different magnetic stirrer, which was set to its maximum of 300 rpm.

Characterization

The presence of organic groups on the nanoparticle surface from silane-modification was determined using FTIR from 400 to 4000 cm^{-1} at a resolution of 2 cm^{-1} (Equinox 55 FTIR, Bruker) on KBr pellets containing 3 wt % sample. The amount of silane present on the nanoparticles was determined using thermogravimetric analysis (TGA) in air from room temperature to 800 $^{\circ}\text{C}$ at 20 $^{\circ}\text{C}/\text{min}$ (2050 TGA, TA Instruments). The average coverage of the silica nanoparticle surfaces by silane molecules, σ , was estimated from the TGA mass loss by assuming an average silica nanoparticle surface area of 390 m^2/g . The mass loss between 25 and 100 $^{\circ}\text{C}$ was associated with the elimination of water and the mass loss between 100 and 200 $^{\circ}\text{C}$ was associated with hydrocarbon contaminants. The mass loss between 200 and 800 $^{\circ}\text{C}$ was ascribed to the pyrolysis of the organic part of the silane (whose molecular weight is known). The TGA data from this temperature range could, therefore, be used to estimate the number of silane molecules per unit area of silica surface. Surface modification using trialkoxysilane was not expected to form monomolecular coverage but rather to form a complex three-dimensional silsesquioxane network. Such networks were found to enhance the thermal and mechanical properties of polymers.^{14–17,48}

The polyHIPE density was determined using gravimetric analysis. The polymerization yield was calculated following drying (but before extraction) by assuming that all the silica, surfactant, initiator, and stabilizer salt added to the HIPE remained within the polyHIPE. The gel content was determined from the mass loss following 48 h in boiling xylene and drying in a vacuum oven. The porous structure was characterized using scanning electron microscopy (SEM) for carbon-coated fracture surfaces (FEI Quanta 200, 5–15 kV) and high resolution SEM (HRSEM) on uncoated fracture surfaces (LEO 982, Zeiss, 3 kV). Average polyHIPE void sizes

were taken from the SEM micrographs and then corrected to take the statistical nature of the cross section into account.⁴⁹

Samples that could undergo ultramicrotomy for TEM specimen preparation were prepared by infiltrating a polyHIPE with MMA containing 1 wt % BPO. The MMA infiltration took place under vacuum for several hours. To enhance the flow of MMA into the sample, a PPHIPE with a relatively high degree of pore interconnectivity was synthesized using toluene as a porogen in the organic phase. This sample has a “T” appended to its name, and its recipe is listed in Table 1. The MMA was polymerized at 50 $^{\circ}\text{C}$ in a circulating air oven. Ultramicrotomy (Ultracut E, Reichert-Jung) was then used to prepare specimens for TEM (FEI Technai G² T20 S-Twin, operating at 200 kV).

RESULTS AND DISCUSSION

Surface Modification

The FTIR spectra of the as-received and of MPtMS-modified silica nanoparticles (r_m of 1.8) are presented in Figure 2. The as-received silica nanoparticles exhibit bands commonly associated with silica, as well as a broad band associated with SiOH and adsorbed water at 3429 cm^{-1} and a broad band associated with adsorbed water at 1629 cm^{-1} . The MPtMS-modified silica nanoparticles exhibit bands in Figure 2 that are associated with the silane and that are not found in the as-received silica nanoparticles. There are bands at 1450 and 2951 cm^{-1} associated with CH_2 and CH_3 groups, a band at 1722 cm^{-1} associated with ester groups, and a narrow band at 1636 cm^{-1} associated with $\text{C}=\text{C}$, which is quite different from the band associated with adsorbed water in the spectrum of the as-received nanoparticles. The ratio of the height of the band at about 1630 cm^{-1} to the height of the band at 3429 cm^{-1} is 0.22 for the as-received nanoparticles and 0.32 for the modified nanoparticles. The enhanced intensity of the normalized band height reflects the presence of both adsorbed water and $\text{C}=\text{C}$ bonds.

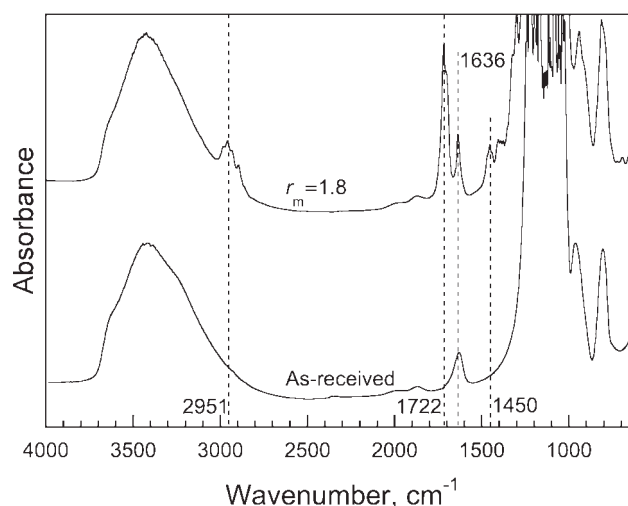


FIGURE 2 FTIR spectra of as-received and MPtMS-modified silica nanoparticles (r_m of 1.8).

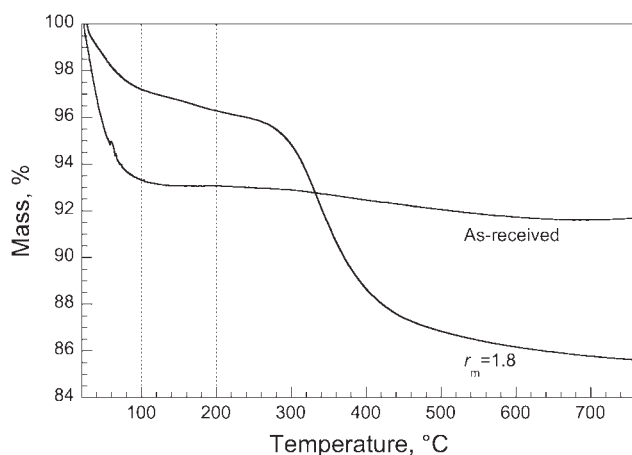


FIGURE 3 TGA curves from as-received and MPtMS-modified silica nanoparticles (r_m of 1.8).

The TGA curves from the as-received and MPtMS-modified silica nanoparticles (r_m of 1.8) are presented in Figure 3. The most significant mass loss for the as-received silica nanoparticles occurs between 25 and 100 °C and is associated with the elimination of water. There is relatively less mass loss between 100 and 800 °C. MPtMS-modification produces a significant reduction in the amount of absorbed water (Fig. 3), indicating that the surface has become more hydrophobic. The mass loss between 100 and 200 °C is relatively small for the MPtMS-modified silica nanoparticles. An increase in the rate of mass loss begins at about 200 °C (Fig. 3). The relatively significant mass loss between 200 and 800 °C is associated with the pyrolysis of the organic part of the silane molecules.

The average surface coverage estimated from the TGA results is presented as a function of MPtMS content in Figure 4. The amount of silane on the nanoparticle surfaces increases in a linear fashion with MPtMS content. The TGA mass losses in the temperature ranges discussed earlier for silica nanoparticles modified with various silanes (r_m of 1.8) are summar-

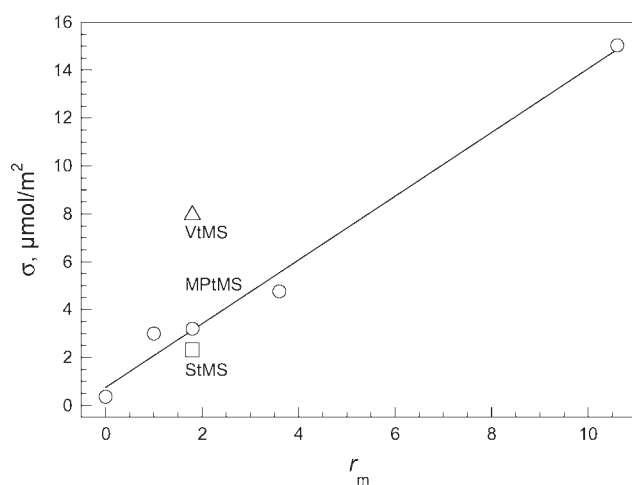


FIGURE 4 The dependence of σ on r_m and on silane chemistry.

TABLE 3 TGA Mass Loss from As-Received and Silane-Modified Silica Nanoparticles (r_m of 1.8)

Silane	TGA Mass Loss (%)			σ ($\mu\text{mol}/\text{m}^2$)
	25–100 °C	100–200 °C	200–800 °C	
None	6.7	0.2	1.4	–
MPtMS	2.9	0.9	10.7	3.2
MPdMS	2.0	0.8	10.0	2.9
AAPtMS	2.2	2.1	11.7	4.2
APtMS	2.7	1.1	10.8	3.8
StMS	3.7	2.2	9.0	2.3
VtMS	2.7	1.7	6.1	8.1

ized in Table 3. All the silane modifications were effective in enhancing the hydrophobicity of the surface, producing similar reductions in the amount of absorbed water. Most of the silane modifications also produce similar molecular coverage, around $3 \mu\text{mol}/\text{m}^2$. VtMS, with its relatively low molecular weight and relatively small organic group, has an exceptionally high surface coverage of around $8 \mu\text{mol}/\text{m}^2$ reflecting the ability of the smaller molecules to pack more efficiently.

Emulsifier-Stabilized PolyHIPE

The emulsifier-stabilized polyHIPE, S0, has a relatively high yield (Table 4). Its density of $0.17 \text{ g}/\text{cm}^3$ reflects its overall monomer content (Table 1). S0 has a porous structure typical of polyHIPE, Figure 5(a), a highly interconnected void structure with an average void diameter of $20 \mu\text{m}$.

Polymerized Pickering HIPES

Stable PPHIPES could only be produced using silane-modified silica nanoparticles. The as-received nanoparticles, which are relatively hydrophilic, did not seem to preferentially locate at the oil–water interface, a necessary condition for the formation of a stable Pickering HIPE. Polymerization within the Pickering HIPE produced white monoliths and a

TABLE 4 PolyHIPE Yields, Densities, and Void Sizes

PolyHIPE	Yield (%)	ρ (g/cm^3)	Voids (μm)
S0	94.8	0.17	20
S0-B	97.3	0.19	10
S4-a1.0	83.1	0.18	60, 175
S4-a1.8	81.8	0.16	60, 115
S4-a1.8-B	64.1	0.15	310
S4-a1.8-T	66.9	0.12	110
S4-a1.8-S	87.7	0.16	60
S4-a3.6	71.9	0.14	55, 315
S7-a1.8	89.5	0.16	150, 300
S4-b1.8	73.6	0.16	135, 250
S4-c1.8	65.7	0.14	365, 635
S4-d1.8	63.9	0.15	315, 680

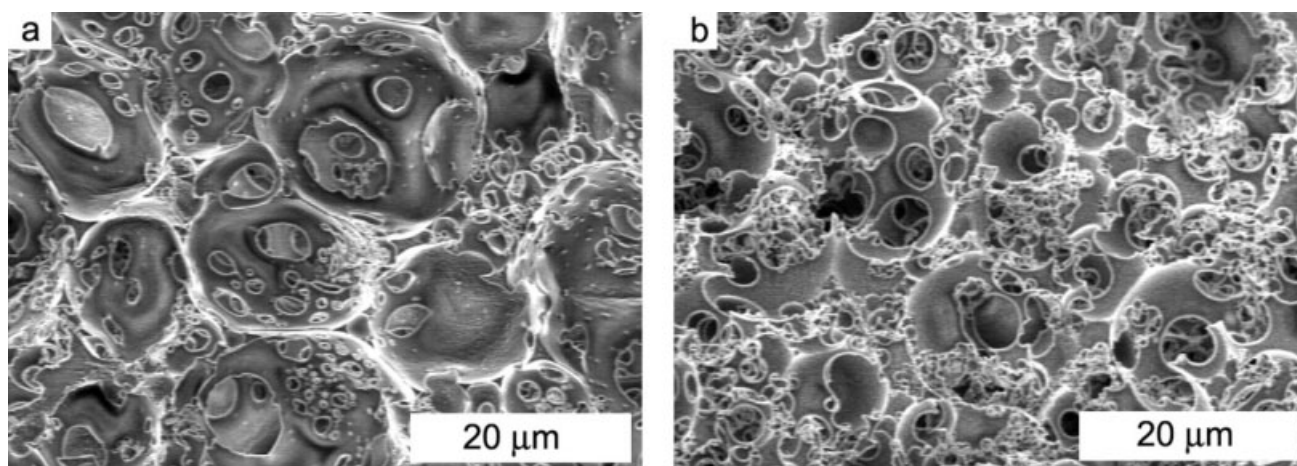


FIGURE 5 SEM micrographs of: (a) S0; (b) S0-B.

negligible amount of shrinkage was observed. The densities of the PPHIPes were around 0.16 g/cm^3 (Table 4).

The PPHIPes exhibited porous structures that were quite different from the highly interconnected micrometer-scale porous structure of typical polyHIPes. The porous structure of a typical PPHIPE consisted of relatively large polyhedral voids with no obvious interconnecting structure [Fig. 6(a,b) for S4-a1.8]. These polyhedral shapes result from the dense packing of relatively monodisperse droplets.¹ The porous structure had a bimodal void size distribution. Most of the polyhedral voids were relatively large, with an average diameter of $115 \mu\text{m}$. A small minority of the polyhedral voids were located between the larger voids and had an average diameter of $60 \mu\text{m}$. The void walls were several micrometers thick, which is relatively thick for a polyHIPE. In spite of the seemingly closed-cell structure, it was possible to remove the water from the internal phase. The ability to remove the water indicates that there is some interconnectivity, perhaps on the nanometer scale, a scale much smaller than the void dimensions.

The effects of several synthesis parameters on HIPE stability and PPHIPE structure were investigated. Each of these parameters could affect nanoparticle migration to the oil-water interface and the formation of a stable structure. A reduction in droplet size is indicative of enhanced interfacial stability.³⁵ The size of the PPHIPE voids is, therefore, indicative of HIPE stability, with smaller voids indicating a more stable HIPE. The extent of surface modification, the nanoparticle content, the chemical nature of the silane, the intensity of mixing, and the locus of initiation could all affect HIPE stability.

Extent of Surface Modification

The hydrophilic/hydrophobic nature of the particles is determined by the extent of surface modification, which is varied through the concentration of silane in the modification process.^{34,35,37} As-received nanoparticles were unable to stabilize a HIPE. These nanoparticles, with their relatively high absorbed water content, are too hydrophilic for HIPE stabiliza-

tion. MPtMS, widely used as a silane coupling agent for glass fibers and successfully used to synthesize interconnected hybrid network polyHIPes, was chosen as the primary silane for this investigation.^{12,13,40} The voids produced using nanoparticles modified with r_m of 1.0 and 3.6 [Fig. 6(c)] were significantly larger (Table 4) than those produced using nanoparticles modified with an r_m of 1.8. Therefore, an r_m of 1.8 was chosen as optimal for this investigation. The silica nanoparticles modified using an r_m of 10.6 produced a relatively high TGA mass loss between 200 and $800 \text{ }^\circ\text{C}$ (Fig. 4) indicating extensive modification. Unexpectedly, these nanoparticles were unable to stabilize a HIPE. The relatively high silane surface coverage rendered these nanoparticles too hydrophobic to preferentially migrate to the oil/water interface and stabilize the HIPE.

Nanoparticle Content

Stable PPHIPes could be produced using silica nanoparticle contents ranging from 2.1% to 7.0% of the monomer mass (r_m of 1.8). There were not enough nanoparticles to form a stable HIPE at nanoparticle contents below 2.1 wt % and, therefore, phase separation occurred. The large amount of interfacial area created with more than 7.0 wt % nanoparticles made the HIPE too viscous to mix. The high viscosity limited mixing and, therefore, limited the amount of internal phase that could be incorporated into the HIPE.² The voids from a HIPE containing 7.0 wt % silica nanoparticles [Fig. 6(d)] were significantly larger (Table 4) than those from a HIPE containing 4.2 wt % silica nanoparticles [Fig. 6(a,b)]. A nanoparticle content of 4.2 wt % was chosen as the optimal silica nanoparticle content for this investigation. The observed increase in HIPE viscosity with increasing silica content has also been observed in emulsifier-stabilized HIPes.^{18,19}

Silane Chemistry

A variety of silane chemistries with different hydrophobicities and reactivities were investigated (Fig. 1). Interestingly, silica nanoparticles modified with MPdMS, a dialkoxysilane bearing the same organic group as MPtMS, were not able to

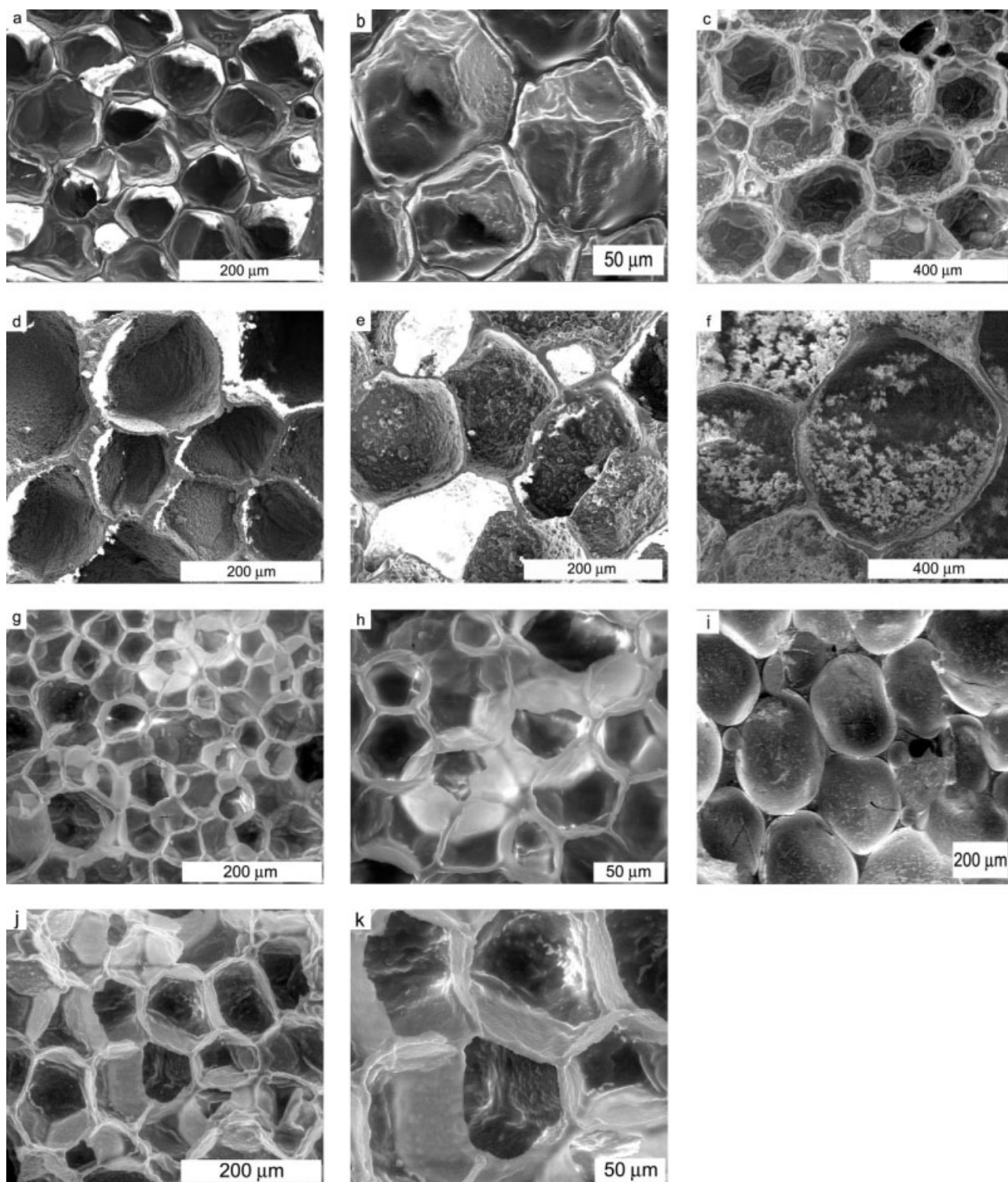


FIGURE 6 SEM micrographs of: (a,b) S4-a1.8; (c) S4-a3.6; (d) S7-a1.8; (e) S4-b1.8; (f) S4-c1.8; (g,h) S4-a1.8-S; (i) S4-a1.8-B; (j,k) S4-a1.8-T.

produce a stable HIPE. This result may indicate the need for the complex silsesquioxane network structure from a trialkoxysilane rather than the more linear structure from a dialkoxysilane. A PPHIPE could be produced using nanoparticles modified with AAPTMS, but the resulting polyHIPE collapsed during drying and could not be studied further.

PPHIPEs were successfully obtained using silica nanoparticles modified with APTMS [Fig. 6(e)], VtMS [Fig. 6(f)], and StMS [similar to Fig. 6(f)]. For all these different silanes, the resulting voids were significantly larger (Table 4) than those produced using MPtMS [Fig. 6(a,b) and Table 4]. The voids produced using APTMS surface modification had an average

diameter of 250 μm , whereas the voids produced using VtMS and StMS were 635 μm and 680 μm , respectively. Both the acrylate (APtMS) and the methacrylate (MPtMS) bear a chemical similarity to the monomer EHA, and this may enhance HIPE stability and yield smaller voids. AAPtMS, VtMS, and StMS are chemically dissimilar to EHA and this may produce a less stable HIPE. APtMS, VtMS, and StMS also exhibit polymer particles deposited on the void walls. These deposits most likely result from emulsion polymerization of monomers within the droplets formed by the internal phase, as seen in other polyHIPE systems.⁵⁰ The amounts of such deposits preclude their being silica nanoparticle agglomerates. Based on these results, MPtMS was chosen as the optimal silane for this investigation.

Mixing Intensity

The extent of mixing a HIPE can affect the porous morphology of a polyHIPE.²² The Pickering HIPE recipe that yielded the smallest voids in the corresponding PPHIPE was also used to produce a Pickering HIPE using more intensive mixing. The porous structure of the less intensely mixed S4-a1.8, Figure 6(a,b), can be compared with that of the more intensely mixed S4-a1.8-S, Figure 6(g,h). The voids in the PPHIPE from the more intensely mixed Pickering HIPE have a similar polyhedral shape as the voids in the PPHIPE from the less intensely mixed Pickering HIPE but are significantly smaller and more uniform, with an average diameter of 60 μm . The increase in shear rate produces an increase in shear stress, reducing the droplet size, increasing the droplet number density, and reducing the wall thickness. The reduction in wall thickness makes the walls more susceptible to ruptures that can occur during polymerization and/or postpolymerization processing, as seen in Figure 6(g,h).

Locus of Initiation

Previous work has demonstrated that changes in the locus of initiation can produce dramatic changes in the porous structure and properties of a polyHIPE.^{51–53} S0-B, the emulsifier-stabilized HIPE initiated with BPO instead of KPS, had a high yield and a density of 0.19 g/cm^3 , similar to those of S0. S0-B had a gel content of 94%, higher than the gel content of 85% for S0. S0-B exhibits a typical polyHIPE structure, with the voids in Figure 5(b) for S0-B having an average diameter of 10 μm , somewhat smaller than the average diameter of 20 μm for S0 in Figure 5(a) (Table 4). Similar amounts of BPO and KPS were added to the HIPEs. However, the KPS was added to the major, aqueous phase, whereas BPO was added to the minor, organic phase. Therefore, the concentration of BPO in the organic phase was significantly higher than the concentration of KPS in the aqueous phase. The higher gel content in S0-B reflects its higher initiator concentration.

The gel contents of the PPHIPEs, 91% for S4-a1.8 and 97% for S4-a1.8-B, are higher than those of the conventional reference polyHIPE. This increase in gel content indicates that there is some copolymerization with the vinyl groups on the surfaces of the nanoparticles. The silane-modified nanoparticles, therefore, also act as crosslinking junctions. As seen

for the reference polyHIPE, the higher initiator concentration in the organic phase yields a higher gel content. The porous structure of S4-a1.8-B [Fig. 6(i)] is quite different from that of S4-a1.8 [Fig. 6(a,b)] in spite of their almost identical recipes. Although S4-a1.8 has polyhedral voids, S4-a1.8-B has spherical voids that are almost thrice as large (Table 4). On heating the HIPE for polymerization, there are two processes that occur simultaneously, polymerization and destabilization. Aqueous-phase initiation is expected to produce a network structure based on high molecular weights and is expected to reach its gel point more rapidly than the network structure based on low molecular weights produced by organic-phase initiation. A smaller droplet size and a polyhedral droplet shape are “locked-in” before extensive destabilization can take place since the aqueous-phase initiated system reaches the gel point more rapidly. The larger, spherical droplets in the organic-phase initiated system reflect the more extensive destabilization that occurs before the system reaches its gel point.

Wall Structure in PPHIPEs

Adding a porogen to the organic phase of a HIPE has been shown to enhance polyHIPE wall porosity without necessarily changing the overall porous structure.¹³ Adding toluene to enhance interconnectivity produced the porous structure in Figure 6(j,k) for S4-a1.8-T. The void sizes and void shapes are quite similar to those in Figure 6(a,b) for S4-a1.8 (Table 4). The walls are thinner by virtue of there being less polymer and are thus more prone to rupture, as seen in Figure 6(j,k). These ruptures bear some similarity to the results from more intensive mixing in Figure 6(g,h). Although the mixture of MMA and BPO could not be easily infiltrated into S4-a1.8, it infiltrated rapidly into S4-a1.8-T.

The internal structure of the void walls within S4-a1.8-T is seen in the cross section TEM micrographs in Figure 7. A P(EHA-co-DVB) polyHIPE void wall (a stripe of light gray) is seen in the center of Figure 7(a) between two PMMA-filled voids (dark gray). There are two rows of silica nanoparticles within the P(EHA-co-DVB) (black lines within the light gray), each one close to the boundary with PMMA, the surfaces of the void walls [marked with arrows in Fig. 7(a)]. The two distinct rows of silica nanoparticles are actually nanoparticle aggregates, as seen in Figure 7(b). This nanoparticle arrangement is to be expected for PPHIPEs. The individual droplets of the dispersed phase are stabilized by a shell of nanoparticles. The close packing of the droplets that occurs in HIPEs brings the nanoparticle shells, each associated with different droplets, quite close together, as illustrated schematically in Figure 8. A cross section of such a structure, immobilized through polymerization, would exhibit two parallel nanoparticle lines, each from a different nanoparticle shell. The nanoparticles are embedded within the P(EHA-co-DVB) walls when they might be expected to be found at the boundary with PMMA, which was originally the oil–water interface. Although the silica nanoparticles may have been at the interface in the original HIPE, the changes in interfacial tension that occur during polymerization could affect their location within the polyHIPE. Copolymerization with the vinyl groups

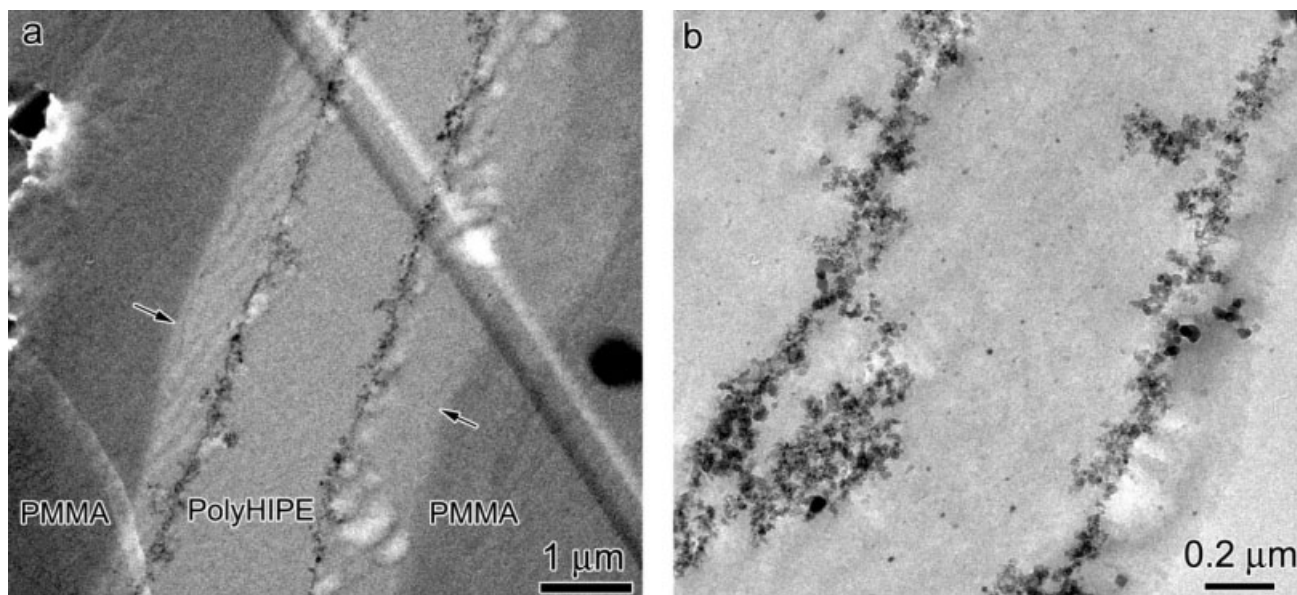


FIGURE 7 TEM micrographs of void wall cross sections from S4-a1.8-T.

on the nanoparticles' surface would produce a polymer coating. This coating would increase nanoparticle hydrophobicity and make them less desirable at the interface. The nanopar-

ticles become embedded in the polymer as monomer migrates to the oil-water interface during polymerization.

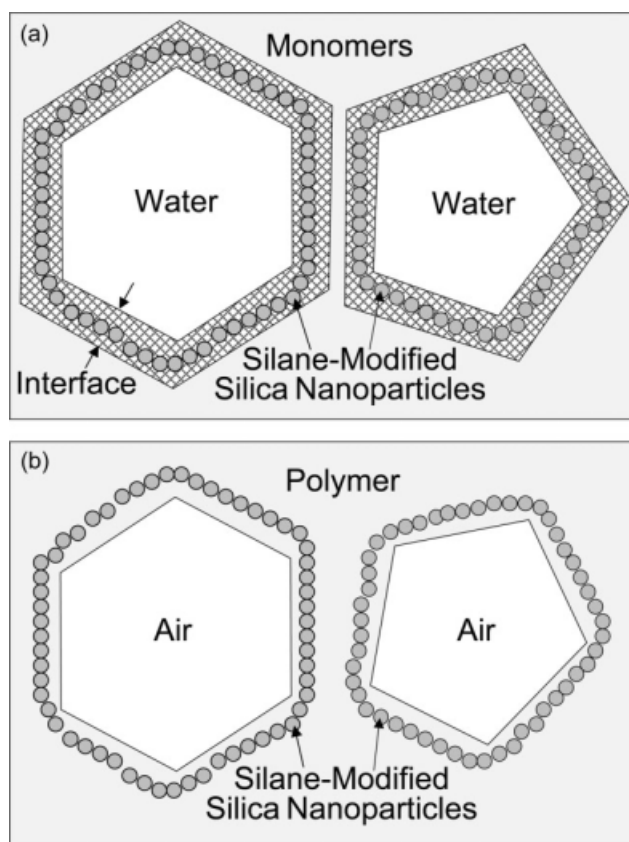


FIGURE 8 Schematic illustration: (a) Pickering HIPE with an assembly of silica nanoparticle shells around the polyhedral droplets of the aqueous phase; (b) polymerized Pickering HIPE.

CONCLUSIONS

Surfactant-free poly(EHA-co-DVB) polyHIPEs were successfully synthesized based on Pickering HIPEs containing silane-modified silica nanoparticles. The silane chemistry and silane content had significant effects on the size of the polyHIPE voids. An MPTMS surface coverage of around $3 \mu\text{mol}/\text{m}^2$ was found to produce the smallest voids, an indication of optimal HIPE stability. The densities and gel contents of the PPHIPEs were similar to those of conventional polyHIPEs. The voids in conventional polyHIPEs are usually spherical, polydisperse, highly interconnected, and around $20 \mu\text{m}$ in diameter. The voids in the aqueous-phase initiated PPHIPE with 4.2 wt % nanoparticles modified using a silane to silica ratio of 1.8 were polyhedral, with a bimodal size distribution and a relatively closed-cell structure. Most of the voids were $115 \mu\text{m}$ in diameter and, situated between them, was a small minority whose diameter was $60 \mu\text{m}$. Increasing the mixing speed produced smaller voids, thinner walls, and enhanced interconnectivity. The locus of initiation had a significant effect on polyHIPE morphology. Organic-phase initiation yielded larger, more spherical voids from the more extensive coalescence before the structure could be "locked-in" at the gel point. Most significantly, the silica nanoparticles were located within the polymer wall rather than, as might be expected, at the interface. The void walls were shown to be an assembly of nanoparticle agglomerate shells that become embedded within the polymer as monomer migrates to the oil-water interface during polymerization.

The partial support of the Israel Science Foundation and of the Technion VPR Fund are gratefully acknowledged.

REFERENCES AND NOTES

- 1 Cameron, N. R.; Sherrington, D. C. *Adv Polym Sci* 1996, 126, 163–214.
- 2 Cameron, N. R.; Sherrington, D. C.; Albiston, L.; Gregory, D. P. *Colloid Polym Sci* 1996, 274, 592–595.
- 3 Williams, J. M.; Wroblewski, D. A. *Langmuir* 1988, 4, 656–662.
- 4 Williams, J. M.; Gray, A. J.; Wilkerson, M. H. *Langmuir* 1990, 6, 437–444.
- 5 Sergienko, A. Y.; Tai, H.; Narkis, M.; Silverstein, M. S. *J Appl Polym Sci* 2004, 94, 2233–2239.
- 6 Sergienko, A. Y.; Tai, H.; Narkis, M.; Silverstein, M. S. *J Appl Polym Sci* 2002, 84, 2018–2027.
- 7 Tai, H.; Sergienko, A.; Silverstein, M. S. *Polym Eng Sci* 2001, 41, 1540–1552.
- 8 Kulygin, O.; Silverstein, M. S. *Soft Matter* 2007, 3, 1525–1529.
- 9 Butler, R.; Hopkinson, I.; Cooper, A. I. *J Am Chem Soc* 2003, 125, 14473–14481.
- 10 Busby, W.; Cameron, N. R.; Jahoda, A. B. C. *Polym Int* 2002, 51, 871–881.
- 11 Lumelsky, Y.; Zoldan, J.; Levenberg, S.; Silverstein, M. S. *Macromolecules* 2008, 41, 1469–1474.
- 12 Tai, H.; Sergienko, A.; Silverstein, M. S. *Polymer* 2001, 42, 4473–4482.
- 13 Silverstein, M. S.; Tai, H.; Sergienko, A.; Lumelsky, Y.; Pavlovsky, S. *Polymer* 2005, 46, 6682–6694.
- 14 Normatov, J.; Silverstein, M. S. *Polymer* 2007, 48, 6648–6655.
- 15 Normatov, J.; Silverstein, M. S. *Macromolecules* 2007, 40, 8329–8335.
- 16 Normatov, J.; Silverstein, M. S. *Chem Mater* 2008, 20, 1571–1577.
- 17 Normatov, J.; Silverstein, M. S. *J Polym Sci Part A: Polym Chem* 2008, 46, 2357–2366.
- 18 Haibach, K.; Menner, A.; Powell, R.; Bismarck, A. *Polymer* 2006, 47, 4513–4519.
- 19 Menner, A.; Haibach, K.; Powell, R.; Bismarck, A. *Polymer* 2006, 47, 7628–7635.
- 20 Menner, A.; Powell, R.; Bismarck, A. *Soft Matter* 2006, 2, 337–342.
- 21 Lepine, O.; Birot, M.; Deleuze, H. *J Polym Sci Part A: Polym Chem* 2007, 45, 4193–4203.
- 22 Richez, A.; Deleuze, H.; Vedrenne, P.; Collier, R. *J Appl Polym Sci* 2005, 96, 2053–2063.
- 23 Deleuze, H.; Faivre, R.; Herroguéz, V. *Chem Commun* 2002, 2822–2823.
- 24 Lepine, O.; Birot, M.; Deleuze, H. *Polymer* 2005, 46, 9653–9663.
- 25 Krajnc, P.; Scarontefanec, D.; Pulko, I. *Macromol Rapid Commun* 2005, 26, 1289–1293.
- 26 Stefanec, D.; Krajnc, P. *React Funct Polym* 2005, 65, 37–45.
- 27 Mezzenga, R.; Ruokolainen, J.; Fredrickson, G. H.; Kramer, E. J. *Macromolecules* 2003, 36, 4466–4471.
- 28 Mezzenga, R.; Fredrickson, G. H.; Kramer, E. J. *Macromolecules* 2003, 36, 4457–4465.
- 29 Mezzenga, R.; Ruokolainen, J.; Fredrickson, G. H.; Kramer, E. J.; Moses, D.; Heeger, A. J.; Ikkala, O. *Science* 2003, 299, 1872–1874.
- 30 Bokhari, M. A.; Akay, G.; Zhang, S.; Birch, M. A. *Biomaterials* 2005, 26, 5198–5208.
- 31 Akay, G.; Birch, M. A.; Bokhari, M. A. *Biomaterials* 2004, 25, 3991–4000.
- 32 Menner, A.; Ikem, V.; Salgueiro, M.; Shaffer, M. S. P.; Bismarck, A. *Chem Commun* 2007, 4274–4276.
- 33 Melle, S.; Lask, M.; Fuller, G. G. *Langmuir* 2005, 21, 2158–2162.
- 34 Binks, B. P.; Lumsdon, S. O. *Phys Chem Chem Phys* 1999, 1, 3007–3016.
- 35 Binks, B. P.; Lumsdon, S. O. *Langmuir* 2000, 16, 8622–8631.
- 36 Binks, B. P.; Clint, J. H. *Langmuir* 2002, 18, 1270–1273.
- 37 Binks, B. P. *Adv Mater* 2002, 14, 1824–1827.
- 38 Binks, B. P.; Fletcher, P. D. I. *Langmuir* 2001, 17, 4708–4710.
- 39 Binks, B. P.; Rodrigues, J. A. *Langmuir* 2003, 19, 4905–4912.
- 40 Plueddemann, E. P. *Silane Coupling Agents*; Plenum Press: New York and London, 1982.
- 41 Jiang, Z. X.; Meng, L. H.; Huang, Y. D.; Liu, L.; Lu, C. *Appl Surf Sci* 2007, 253, 4338–4343.
- 42 Matinlinna, J. P.; Lassila, L. V. J.; Vallittu, P. K. *Dent Mater* 2007, 23, 1173–1180.
- 43 Abboud, M.; Turner, M.; Duguet, E.; Fontanille, M. *J Mater Chem* 1997, 7, 1527–1532.
- 44 Ikem, Vivian O.; Menner, A.; Bismarck, A. *Angew Chem Int Ed Engl* 2008, 47, 8277–8279.
- 45 Menner, A.; Verdejo, R.; Shaffer, M.; Bismarck, A. *Langmuir* 2007, 23, 2398–2403.
- 46 Colver, P. J.; Bon, S. A. F. *Chem Mater* 2007, 19, 1537–1539.
- 47 Zhang, S.; Chen, J. *Chem Commun* 2009, 2217–2219.
- 48 Amir, N.; Levina, A.; Silverstein, M. S. *J Polym Sci Part A: Polym Chem* 2007, 45, 4264–4275.
- 49 Carnachan, R. J.; Bokhari, M.; Przyborski, S. A.; Cameron, N. R. *Soft Matter* 2006, 2, 608–616.
- 50 Cohen, N. Private Communication.
- 51 Livshin, S.; Silverstein, M. S. *Macromolecules* 2007, 40, 6349–6354.
- 52 Livshin, S.; Silverstein, M. S. *Macromolecules* 2008, 41, 3930–3938.
- 53 Gitli, T.; Silverstein, M. S. *Soft Matter* 2008, 4, 2475–2485.